Available online at www.sciencedirect.com
SCIENCE DIRECT®
Earth and Planetary Science Letters 222 (2004) 333–348
EPSL Frontiers
www.elsevier.com/locate/epsl

Frontiers

The importance of ocean temperature to global biogeochemistry

David Archer[a,*], Pamela Martin[a], Bruce Buffett[a], Victor Brovkin[b], Stefan Rahmstorf[b], Andrey Ganopolski[b]

[a] *Department of the Geophysical Sciences, University of Chicago, Chicago, IL 60637, USA*
[b] *Potsdam Institute for Climate Impact Research, P.O. Box 601203, 14412 Potsdam, Germany*

Received 3 December 2003; received in revised form 5 March 2004; accepted 10 March 2004

Abstract

Variations in the mean temperature of the ocean, on time scales from millennial to millions of years, in the past and projected for the future, are large enough to impact the geochemistry of the carbon, oxygen, and methane geochemical systems. In each system, the time scale of the temperature perturbation is key. On time frames of 1–100 ky, atmospheric CO_2 is controlled by the ocean. CO_2 temperature-dependent solubility and greenhouse forcing combine to create an amplifying feedback with ocean temperature; the $CaCO_3$ cycle increases this effect somewhat on time scales longer than ~5–10 ky. The CO_2/T feedback can be seen in the climate record from Vostok, and a model including the temperature feedback predicts that 10% of the fossil fuel CO_2 will reside in the atmosphere for longer than 100 ky. Timing is important for oxygen, as well; the atmosphere controls the ocean on short time scales, but ocean anoxia controls atmospheric pO_2 on million-year time scales and longer. Warming the ocean to Cretaceous temperatures might eventually increase pO_2 by approximately 25%, in the absence of other perturbations. The response of methane clathrate to climate change in the coming century will probably be small, but on longer time scales of 1–10 ky, there may be a positive feedback with ocean temperature, amplifying the long-term climate impact of anthropogenic CO_2 release.

Keywords: carbon cycle; climate; ocean temperature

1. Introduction

The mean temperature of the ocean has varied by more than 10 °C over the past 65 My. The mean ocean temperature in a coupled climate model is roughly as sensitive to pCO_2 as is the mean surface temperature of the earth [1]. Such large changes in temperature must impact biogeochemical cycling in the ocean and atmosphere. In this paper, we consider the implications of the temperature sensitivity of dissolved gases O_2 and CO_2 and methane in clathrate deposits below the seafloor within the context of Cenozoic climate change. The mechanism and extent of the interaction between these systems and temperature depends strongly on the duration of the change in ocean temperature. The largest temperature changes inferred from the geologic record took place on the 10-My time scale, which is long enough to allow weathering feedbacks to imprint their signatures. The glacial cycles are faster than silicate or

* Corresponding author. Tel.: +1-773-702-0823; fax: +1-773-702-9505.
E-mail address: d-archer@uchicago.edu (D. Archer).

0012-821X/$ - see front matter © 2004 Elsevier B.V. All rights reserved.
doi:10.1016/j.epsl.2004.03.011

organic carbon weathering time scales but do interact with the $CaCO_3$ cycle. The response time for changing deep-ocean temperature is about a millennium, so we will not be concerned with time scales shorter than that.

Terminology

ΔT_{2x}: The temperature change resulting from a doubling of the CO_2 concentration of the atmosphere. This term is used in an atypical way in this paper, to describe the mean ocean temperature, rather than the mean surface temperature.

AABW: Antarctic bottom water. A source of surface water to the deep, originating in the Southern Ocean.

Clathrate: Water frozen into a cage structure trapping a gas molecule. Ocean margin sediments contain huge amounts of methane trapped in clathrate deposits. These are also known as hydrates.

Foraminifera: Single-celled $CaCO_3$-secreting heterotrophic protista. The chemistry of their shells provides information about the chemical and physical conditions in which they grew. Planktontic foramifera lived near the sea surface; benthic foraminifera lived on the seafloor.

Gton: 10^9 metric tons, used here exclusively to measure carbon (not CO_2).

LGM: Last Glacial Maximum, 21–18 ky.

NADW: North Atlantic deep water. A source of water carrying the chemical imprint of the surface ocean into the deep.

PETM: Paleocene Eocene Thermal Maximum, an excursion of $\delta^{13}C$ and $\delta^{18}O$ that is generally interpreted as an abrupt warming and release of isotopically light methane from ocean clathrate deposits.

Radiative equilibrium: The balance between influx and output of energy from the planet. With an increase in greenhouse trapping of outgoing infrared light from the surface, the surface temperature must increase to maintain radiative equilibrium.

2. The record of deep-ocean temperature

2.1. Methods

2.1.1. $\delta^{18}O$

The primary tool for reconstructing deep ocean temperature is the stable oxygen isotopic composition ($\delta^{18}O$) of the calcite shells of foraminifera [2–4]. The temperature dependence varies somewhat for different species and across the full range of ocean temperature, but for benthic foraminifera, the response is $\sim 0.25‰$ per °C, relative to a precision in measurement of $\sim \pm 0.02‰$ and a change in $\delta^{18}O$ of $\sim 5.5‰$ over the past 65 My. Reconstruction of temperatures from $\delta^{18}O$ is complicated by a correlation between local salinity and $\delta^{18}O$ in seawater, and by whole-ocean shifts in $\delta^{18}O$ reflecting storage in isotopically light continental ice sheets. The earth was probably ice-free before the late Eocene, 40 My, so this issue affects the more recent part of the record. However, the older part of the record is more affected by calcite recrystallization, which biases the reconstructed temperature toward the colder pore waters [5,6].

2.1.2. Mg/Ca ratio in $CaCO_3$

The Mg/Ca ratio of biogenic calcites increases exponentially with temperature. While the relationship probably has thermodynamic underpinnings, biogenic calcite carries a species-dependent overprint [7,8] which must be determined by empirical calibration [7,9]. Most low-Mg foraminifera used in paleoceanographic studies have a Mg/Ca response of ~ 9–10% per °C, relative to an analytic precision of better than 2% and variation in Mg/Ca of more than 50% over the Cenozoic [10,11].

The concentrations of Mg and Ca ought to have been relatively stable over several million years, but on the 40-million-year time scale of the Cenozoic, ocean chemistry is less certain, and the calibration of extinct species of foraminifera becomes more difficult [10–12]. Calcite solubility increases with Mg content, so that partial dissolution tends to deplete Mg, biasing the reconstructed temperature cold [13]. In spite of these difficulties, Mg paleothermometry is useful for separating ice volume effect in the $\delta^{18}O$ record.

2.2. My time scale changes

The temperature of the deep sea has changed considerably over the last 65 million years (see Fig. 1). The lack of evidence for ice sheets prior to the end of the Eocene suggests that $\delta^{18}O$ primarily reflects temperature during that time. Deep-ocean temperature appears to have been around 8 °C at the start of the Paleocene, warming to a Cenozoic maximum of nearly 12 °C in the early Eocene (~ 50 Ma). Both Mg/Ca and $\delta^{18}O$ indicate a steady cooling throughout the Eocene of ~ 5–7 °C, culminating in an additional abrupt cooling to ~ 4 °C coincident with the development of Antarctic Ice Sheets that persisted during most of the Oligocene [10,14]. The $\delta^{18}O$ records imply a warming with the temporary waning of 'permanent' Antarctic Ice Sheets in the late Oligocene [15]. Mg/Ca, however, suggests that the cold temperatures persisted through the middle to late Miocene [10,11] and possibly until the middle Pliocene [11], with temperature fluctuations of around 1–2 °C persisting on time scales of millions of years. Most of the records suggest a rapid, steady cooling to the present mean ocean temperature of 1.5 °C over the last 5–10 million years. Both $\delta^{18}O$ and Mg/Ca show a ~ million-year warming event around 10 Ma, the Mid-Miocene Climatic Optimum. There are also several ~ 100,000-year spikes in the Cenozoic deep temperature record, the most well-defined spike, a warming event called the Paleocene/Eocene Thermal Maximum, is often attributed to the release of methane from hydrates.

2.3. Millennial to glacial time scale changes

Temperature cycles are also documented on shorter, glacial/interglacial time scales (Fig. 2). Interpretation of $\delta^{18}O$ is complicated by large changes of ice volume; but the emerging consensus is that half of the ~ 2 ‰ $\delta^{18}O$ change from full glacial to interglacial conditions during the Pleistocene is due to ice, and the other half reflects a temperature change of at least 3 °C with deep-ocean temperature dropping below − 1 °C. This is consistent with evidence from benthic Mg/Ca records for the Quaternary [13,16] and deep core pore water reconstructions for the Last Glacial Maximum [17,18]. Comparison of ice core records and deep-sea geochemical records suggests that there is a strong 100,000 component of deep-sea temperature change, but the deep-sea records also show fluctuations on the order of 2 °C associated with the higher frequency Milankovitch cycles (41 and 23 ky) [13,19]. At an even higher resolution, Mg/Ca and $\delta^{18}O$ records from moderate sedimentation rate deep-sea cores imply short warming events of 0.5–1.5 °C on the order of several thousand years during the last glacial, consistent with comparison of $\delta^{18}O$ records and high-resolution records of sea level change reconstructed from coral reefs [20].

3. Mechanisms of ocean temperature change

3.1. My time scale

On the longest time scales, the mechanism by which the deep-ocean temperature achieves the warmest observed levels is something of a mystery. The central issue is whether the ocean flips from its present dominantly temperature-driven to a salinity-driven overturning circulation, or alternatively if temperature-driven circulation can generate the observed warming. Salt-driven circulation would lead naturally to warmer deep-ocean temperatures, as the sites of convection move to lower latitudes. The coupled atmosphere/ocean simulations of the Eocene from Huber and Sloan [21] were described as "quasi halothermal" circulation. Deep-water formation took place in a cool (~ 9 °C) but salty subpolar North Atlantic. The deep-ocean temperature in these simulations reached 6 °C above modern, at the lower end of Eocene deep temperature reconstructions. Higher atmospheric pCO_2 than their assumed 560 μatm would help to get a warmer deep ocean, but perhaps at the expense of excessive tropical warming. The simulation of Zhang et al. [22,23] achieved a true salt-driven overturning circulation, with much higher deep-ocean temperatures, but their simulation was unstable to occasional temperature-driven deep sea purges, and thus the temperature of the deep sea oscillated between a range of 10–16 °C.

3.2. Millennial to glacial time scale

On shorter, glacial/interglacial time scales, the observed temperature changes are somewhat easier to explain. Deep convection continues to occur at high latitudes. On the one hand, surface temperature

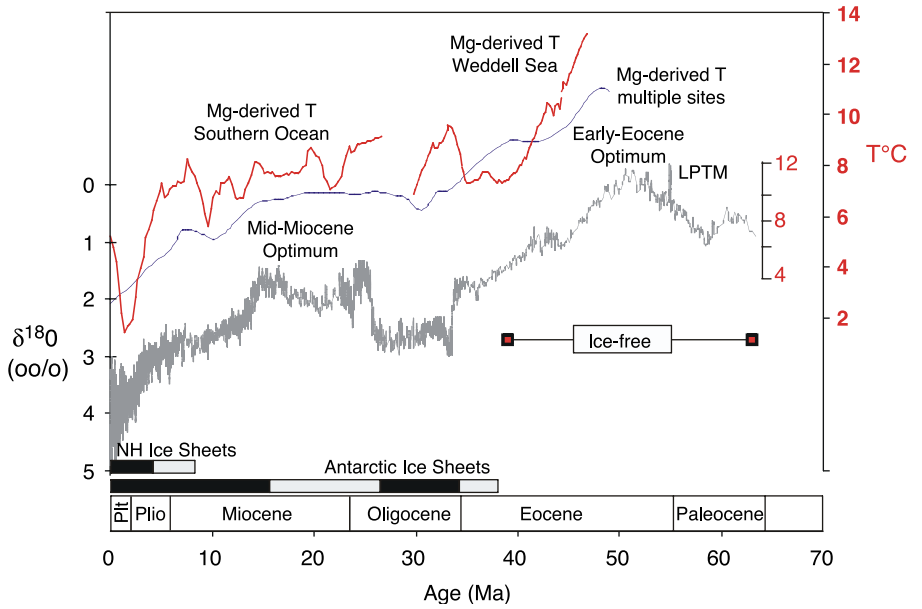

Fig. 1. Comparison of the benthic foraminiferal composite oxygen isotope record for the Cenozoic [14] (bottom gray line) and smoothed Mg/Ca derived temperature records (red and blue lines) [10,12]. The blue line is derived from Mg/Ca of multiple genera of benthic foraminifera from several, disparately located cores [10]. The red line from 0 to 26 Ma represents the temperatures derived from the Mg/Ca record from site 747 (77°E, 55°S, 1695 m) [11]. The red line from ~30 to 50 Ma represents the temperatures derived from the Mg/Ca record from site 689 (3°E, 65°S, 2080 m) [11]. The left axis is scaled for the oxygen isotope record. The right axis is scaled to temperature based on the temperature equations of Lear et al. [10] and Martin et al. [13]. Prior to ~40 Ma, the $\delta^{18}O$ record is thought to primarily reflect changes in deep-water temperature. A temperature scale is inset to estimate the cooling implied by the oxygen-isotoped data based on the temperature equation of Shackleton [4]. Banding on the lower left represents ephemeral (gray) and permanent (black) ice sheets in Antarctica (bottom) and the Northern Hemisphere (modeled after Zachos et al. [14]).

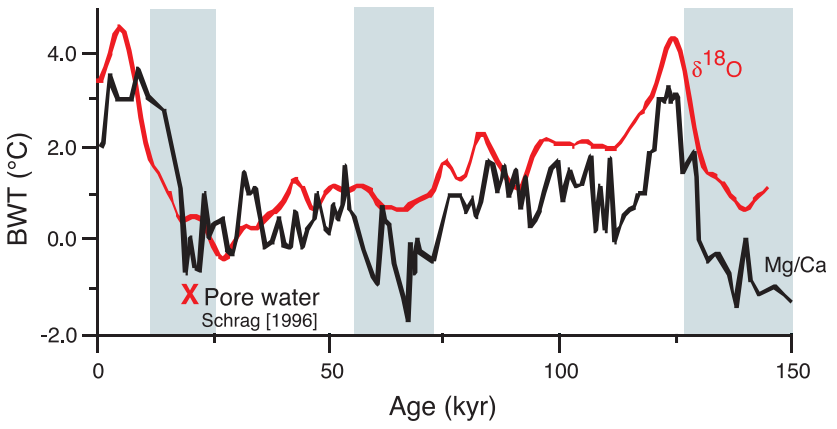

Fig. 2. Bottom water temperature changes over the last two glacial cycles for the deep tropical Atlantic. The red line is the temperature record from M12392 (25°N, 17°W, 2573 m) derived from regional comparison of $\delta^{18}O$ records [59]. The black line is the Mg-derived bottom water temperature from M16772 (1°S, 12°W, 3912 m) [13]. The 'X' is the temperature at the last glacial maximum derived from pore water $\delta^{18}O$ measurements. Figure adapted from Martin et al. [13].

changes there are larger than at low latitudes because of the ice albedo feedback. On the other hand, deep convection tends to occur near the sea ice edge and can shift in location with the ice edge, which tends to stabilize the temperature at which deep water forms.

The mechanism for glacial cooling of the deep ocean beyond its already cool modern mean of 1.5 °C probably derives from the North Atlantic, where North Atlantic Deep Water (NADW) currently warms the deep ocean with a steady stream of 4 °C water. During glacial time, Glacial NADW (GNADW) was colder than at present and formed further to the south [24,25]. Because deep water masses of southern origin are close to the freezing point and could not cool much farther, the increased density of colder Glacial North Atlantic Deep Water (GNADW) would by itself push the boundary between northern and southern component waters in the Atlantic deeper, in contrast to proxy observations [26]. However, a salinity increase in Antarctic Bottom Water (AABW) and a decrease in GNADW [18,26], driven perhaps by an increase in sea ice export from the Antarctic [27], may compensate for the cooler GNADW in the glacial ocean [27].

The cooling of the glacial climate was the combined result of lowered CO_2 and higher planetary albedo due to large ice sheets. For the effect of CO_2 alone on deep-sea temperature, we can turn to the coupled modeling results of Stouffer and Manabe [1]. They found that deep-sea temperature increased by about 3 °C for doubling CO_2, in a range of 0.5–4 times a 300 μatm reference level. That is to say, deep-ocean temperature changes roughly follow changes in the mean temperature of the surface of the earth. The time constant for changing deep-ocean temperature in these simulations is about 1000 years for cooling, and about twice as long for a warming. The maximum predicted increase in deep-ocean temperature was about 6.5 °C under a $4 \times CO_2$ atmosphere, and cooling by 3 °C under $0.5 \times CO_2$.

4. Chemical impacts of ocean temperature

4.1. CO_2

4.1.1. Millenial time scale

The ocean is a larger reservoir for CO_2 than is the atmosphere, so on time scales of 1–100 ky, the relative variability of the CO_2 concentration of the ocean is smaller than that of the atmosphere. In addition to ocean temperature, atmospheric pCO_2 on this time scale is affected by biological redistribution of carbon in the ocean (the biological pump) and other factors. The relationship between ocean temperature and atmospheric pCO_2 is interesting, though, because CO_2 is affected by T and T is affected by CO_2 simultaneously [16].

The two relationships between temperature and CO_2 are radiative equilibrium and CO_2 solubility. We approximate these relationships as linear sensitivities about the present-day condition, although in reality, the solubility of CO_2 is exponential in temperature, and radiative equilibrium temperature goes as the log of the CO_2. Radiative equilibrium is also amplified by the ice albedo feedback, which becomes larger as it gets colder. We will facilitate direct comparisons of these relations by expressing both in a common metric of $\Delta CO_2/\Delta T$.

The radiative equilibrium relationship of concern to us here is the impact of CO_2 as a greenhouse gas on the mean temperature of the ocean. As described above, model simulations [1,28] and data from glacial time [16,18] indicate that changes in the deep-sea temperature roughly parallel those of the mean earth's surface. Based on an assumed value of the climate sensitivity to doubling CO_2, ΔT_{2x}, of 3 °C, and assuming that mean ocean temperature follows mean surface temperature, we would expect CO_2/T to covary with a slope of about 50–70 μatm/°C, depending on the magnitude of the pCO_2 change (because we are linearizing an exponential). In the direction of cooling, the magnitude of the slope decreases; the transition from glacial to interglacial climate was driven by ice albedo forcing as well as changes in CO_2, resulting in a slope of covariation of approximately 30 μatm/°C.

The other relationship is the solubility of CO_2. Simple thermodynamics of a homogeneous seawater sample with no circulation or biological pump yields a pCO_2 sensitivity of 4.23% pCO_2/°C, which translates to $\sim$ 10 μatm/°C. All of the box models and GCMs tested by Martin [16] exhibited similar or slightly smaller slopes of covariation than this, as do new model results presented below.

If we depict the radiative (R) and solubility (S) relations as lines on a pCO_2/T diagram (Fig. 3a), the

ocean temperature and atmospheric pCO_2 find the intersection of these two lines, satisfying the radiative equilibrium and CO_2 solubility constraints simultaneously. This takes place on time scales of the ventilation of the deep sea, order of 1 ky. A source of CO_2 to the system, or an external forcing of temperature, manifests itself as a change in the position of one of the two lines, driving the system to find the new intersection.

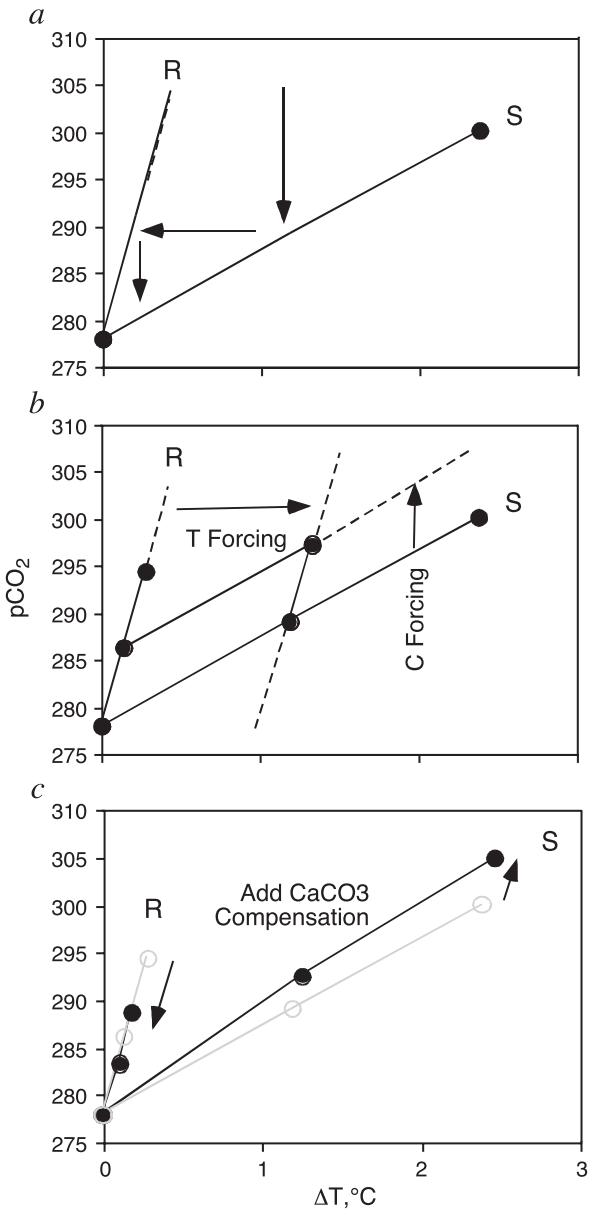

We demonstrate this idea using the Hamocc2 ocean carbon cycle coupled to a simple $CaCO_3$ sediment model [29–31]. To this model, we imposed a uniform whole-ocean temperature sensitivity to atmospheric pCO_2 of the form

$$\Delta T_{\text{ocean}} = 3\,^{\circ}\text{C}/\ln(2) \cdot \ln(pCO_2/278) \quad (1)$$

where 3 °C is from [1] and is a typical value for ΔT_{2x}, the climate sensitivity (the range of uncertainty given for this value in IPCC 2001 is 1.5–4.5 °C). Hamocc2 is an offline tracer advection model, so that changes in temperature affect the solubility of CO_2 but not the circulation.

The results in Fig. 3b arise from two types of perturbation experiments, representing externally driven changes of either temperature or CO_2. We perturb CO_2 by adding 100 or 200 Gtons C as CO_2 to the atmosphere, and running to equilibrium after 6000 years. The added CO_2 partitions itself between the atmosphere and the ocean, with its solubility modified by the change in temperature due to increased atmospheric pCO_2. Because we are adding CO_2 by means other than changing the ocean temperature, this perturbation has the effect of moving the solubility relation vertically on Fig. 3b, in a direction of increasing CO_2 at unchanging temperature. The CO_2/T system then finds the intersection of the radiative and the modified solubility relationship. The solubility line moves with CO_2 addition, but the radiative line does not. The results of several CO_2 addition experiments trace out the location and slope

Fig. 3. (a) Temperature and CO_2 forcing experiments in the Hamocc2 ocean carbon cycle model are used to determine the interaction between the radiative equilibrium and solubility relationships between deep-ocean temperature and atmospheric pCO_2. Temperature as a function of CO_2, or radiative equilibrium, denoted by "R" in the figure, is hard wired into the ocean model, as a uniform temperature offset from a present-day annual mean model result according to ΔT_{2x} of 3 °C. (b) The "R" relationship is found by adding 100 or 200 Gtons of CO_2 to the atmosphere and running to equilibrium. The CO_2 solubility or "S" relationship is found by perturbing the ocean temperature by 1 or 2 °C and allowing CO_2 to equilibrate. The R and S relationships combine into a positive feedback which amplifies any external perturbation of T or CO_2 by ~ 19%. (c) When $CaCO_3$ compensation is added to the ocean carbon cycle model, the R and S relationships are altered somewhat, and the amplification increases to ~ 24%.

of the radiative relation. For small pCO_2 changes, order of 10 μatm, the slope of this relation is about 60 μatm/°C.

We perturb the temperature by adding a uniform offset to the temperature field when calculating the solubility of CO_2. The change in temperature causes CO_2 to degas, increasing the ocean temperature a bit further according to Eq. (1). Because we are altering temperature by means other than changing atmospheric pCO_2, the T forcing perturbation offsets the radiative relation horizontally on Fig. 3b, in the direction of increasing temperature at constant pCO_2. The new intersection of the two relations therefore traces out the trajectory of the solubility relation. The slope of the solubility relation is predicted to be about 9–10 μatm/°C.

Either type of perturbation provokes a positive feedback; for example, externally forced warming drives a CO_2 degassing which warms the ocean a bit further. The magnitude of the feedback depends on the relative slopes of the two relations. We linearize the radiative relation as

$$C = \alpha_R T(C) + r$$

where C is the atmospheric pCO_2, $T(C)$ is temperature as a variable dependent on CO_2, r is some offset, and α_R is the radiative slope, the inverse of the climate sensitivity, estimated above to be 60 μatm/°C above. The linearized solubility relation is

$$C(T) = \alpha_S\ T + s$$

where $C(T)$ is CO_2 but now dependent on T, s is an offset, and α_S is estimated above to be 10 μatm/°C. Then the simultaneous solution (the intersection of the two relations) is

$$T = (s - r)/(\alpha_R - \alpha_S).$$

This solution is stable for $\alpha_R > \alpha_S$; in the reverse case, the feedback is unstable and a runaway CO_2 degassing results. If we make an initial temperature perturbation ΔT, this is equivalent to offsetting the radiative line horizontally by a distance ΔT. This requires a change in r given by

$$\Delta r = \alpha_R \Delta T.$$

The final change in temperature, after the feedback, is given by

$$\Delta T_{final} = \Delta r \delta T/\delta r = \alpha_R \Delta T_{forcing}/(\alpha_R - \alpha_S)$$

and rearranging,

$$\Delta T_{final} = \Delta T_{forcing}(1 + \alpha_S/(\alpha_R - \alpha_S))$$

where the extent of amplification factor is represented by the term $\alpha_S/(\alpha_R - \alpha_S)$. For the values of α_R and α_S estimated above, this positive feedback comes to about 18–20%. For example, an initial temperature forcing of 1°C will generate an ultimate temperature change, after the CO_2 feedback, of 1.2°C.

4.1.2. Glacial time scale

On time scales of the glacial cycles (from 5 to 200 ky) the alkalinity and $CaCO_3$ cycles regulate the pH of the ocean, affecting the pCO_2 of the atmosphere. The fundamental constraint in the ocean is a balance between the influx of dissolved $CaCO_3$ and its removal by burial in sediments, called $CaCO_3$ compensation. Externally driven fluctuations in pCO_2, such as by changes in the biological pump or fossil fuel combustion, are damped by $CaCO_3$ compensation. However, $CaCO_3$ compensation adds a new sensitivity to the carbon cycle, the weathering and production of $CaCO_3$ [32].

The concentration of Ca^{2+} exceeds that of $CO_3^{=}$ by several orders of magnitude, and its residence time is longer despite a slight buffering of $CO_3^{=}$ by HCO_3^- and CO_2. The ocean therefore uses $CO_3^{=}$ as the regulator of $CaCO_3$ burial. If $CaCO_3$ burial is slower than weathering, for example, dissolved $CaCO_3$ builds up in the ocean, increasing $CO_3^{=}$, until burial equals weathering.

$CaCO_3$ compensation has a small but noticeable effect on the CO_2 and T feedbacks (Fig. 3c) by buffering the CO_2 concentration of the atmosphere against external sources and sinks. A 100-Gton CO_2 addition initially increases pCO_2 by 8 μatm, but $CaCO_3$ compensation ameliorates the atmospheric response to 5 μatm ("R" response, Fig. 3c). In addition, the solubility relation sensitivity is increased by $CaCO_3$ compensation, from about 9–10 μatm/°C to about 11–12 μatm/°C. This can be

understood from the following chain of events. An increase in ocean T causes CO_2 to degas, decreasing ocean CO_2 and therefore shifting the pH of the ocean toward the basic. As a result, ocean $CO_3^=$ increases, roughly proportionally to the CO_2 decrease. $CaCO_3$ compensation, by insisting on equilibrium with $CaCO_3$, restores $CO_3^=$ toward its original value, and as $CO_3^=$ falls, the pH of the ocean shifts back toward the acidic and atmospheric pCO_2 rises still a bit further. Using the $CaCO_3$ compensation value for α_S, we calculate a feedback amplitude of about 23–25% for the CO_2/T relation, on time scales of 5–10 ky. This same feedback amplitude applies to perturbations of CO_2 or T.

4.1.3. Impacts of the CO_2/T feedback

The effects of the CO_2/T relation can be read in the tea leaves of the Vostok ice-core record [33]. The large CO_2 transition at the deglaciation is difficult to take apart, because everything is happening at once. Sea level is rising, dust fluxes are dropping, and temperatures are rising. The onset of glaciation is simpler. The Vostok record implies that, the Laurentide ice sheet nucleated at the end of MIS 5e ($\sim$120 ky before present), although atmospheric pCO_2 was high at that time. In ongoing simulations with CLIMBER-2, an Earth system model of intermediate complexity (see Ganopolski et al. [24] for model description), the small ice sheet has a minor effect on climate except for the Northern high latitudes. That is, sea level drop is minor, and yet atmospheric pCO_2 begins to drop (Ganopolski, work in progress). We hypothesize that the North Atlantic is a plausible route to cooling the deep ocean, explaining the initial CO_2 drawdown as a response to ocean cooling. The Mg-derived temperature record shows a deep ocean decrease of 2–3 °C over 10–20 ky on the 5e-4 transition, explaining potentially 30–45 μatm of CO_2 drawdown. After this initial drawdown, changes in sea level, iron fluxes, and planktonic functional groups can be invoked to explain the rest of the drawdown to LGM levels [34].

The CO_2/T relation can also be seen in correlated spikes in CO_2 and T during stage 3. Martin [16] estimated that the slope of the CO_2/T relation during these times was $\sim$10 μatm/°C, similar to the model solubility relation.

The ocean temperature feedback will affect the atmospheric residence time and eventual fate of fossil fuel CO_2 in the future as well. This effect was not considered by [30,31], who used the same model as we are using here to forecast the dynamics of fossil fuel neutralization over a time scale of tens of thousands of years. A comparison of their model with and without the temperature feedback is shown in Fig. 4 and summarized in Table 1. The temperature feedback in this case is applied with a 1000-year relaxation time to a target temperature

$$\Delta T_{\text{target}} = 3\,^{\circ}\text{C}/\ln(2)\cdot\ln(pCO_2/278)$$

using

$$\delta\Delta T_{\text{ocean}}/\delta t = 10^{-3}\ \text{year}^{-1}(\Delta T_{\text{target}} - \Delta T_{\text{ocean}}).$$

The impact of the temperature feedback is to increase the long-term fraction of fossil carbon in the atmosphere. Dissolution in the ocean removes most of the fossil fuel CO_2 on an e-folding time scale of $\sim$300 years, but the temperature feedback increases the fraction of the carbon that resides in the atmosphere for longer than that, by about 20–21%, consistent with the feedback analysis above. Some fraction of the CO_2 remains in the atmosphere even after neutralization with $CaCO_3$; and this fraction also increases when the temperature feedback is included, from $\sim$7% to $\sim$9%, an increase of 23–29%. The mean atmospheric residence time of fossil carbon increases by 20–30% over the case with no temperature feedback, to 40–50 ky.

4.1.4. My time scale

On time scales of 400 ky and longer, atmospheric pCO_2 is controlled by the silicate weathering cycle. The fundamental balance is between degassing of CO_2 from the earth and the uptake of CO_2 by reaction with igneous rocks, mainly the CaO component [35]. This balance between reaction rates is achieved by modulating the pCO_2 of the atmosphere, which mainly affects weathering rates indirectly through variations in the hydrological cycle. It takes a million years or less to achieve the silicate weathering balance [36–38]. On this time scale, the pCO_2 of the atmosphere controls the carbon concentration of the ocean. Most of the interesting changes in

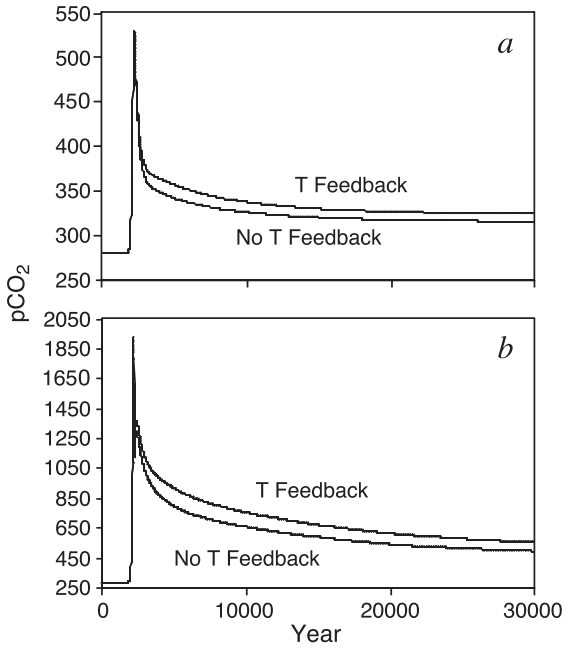

Fig. 4. Long-term fate of fossil fuel CO_2 with and without the ocean temperature feedback. (a) 1000 Gtons C addition experiment, and (b) 5000 Gtons C addition experiment.

carbon chemistry are due to factors other than ocean temperature.

4.2. Oxygen

4.2.1. Millenial to glacial time scale

The direct effect of warming the ocean to a maximum of 12 °C in the early Eocene would be to decrease the saturation O_2 concentration by about 25%. The O_2 content of the atmosphere is approximately 3.6×10^{19} moles, while the O_2 capacity of the ocean, at 4 °C, is two orders of magnitude smaller than this, 3.6×10^{17} moles. Because the atmosphere contains more oxygen than the ocean does, the short-term effect of changing the ocean temperature *T* would be to decrease O_2 in the ocean without changing the concentration in the atmosphere very much. For example, an increase in ocean temperature by 1 °C would decrease the solubility by about 2.6%. O_2 concentrations in the deep ocean are lower than saturation because of biological uptake, but assuming that the biological uptake remains constant, warming the ocean by 1 °C would decrease the ocean inventory by 9.4×10^{15} moles, increasing O_2 in the atmosphere by only 0.026%.

During the Last Glacial Maximum, cooler deep-ocean temperatures would have increased the solubility of oxygen by approximately 10%. The significance of this to the glacial research community is that one candidate for decreasing atmospheric pCO_2 is an increase in the biological pump, which would sequester CO_2 in the deep ocean, along with a corresponding decrease in O_2. As best we can tell, however, the O_2 concentration increased in the present-day oxygen minimum zone [39–41]. Increased solubility of oxygen, aided perhaps by a change in the pattern of intermediate water ventilation, may help the research community explain this observation.

4.2.2. My time scale

On time scales of millions of years, the presence of O_2 in the ocean may be the switch in a chemostat which controls pO_2 in atmosphere. Anoxic sediments are more efficient than oxic sediments at preserving and burying organic carbon, rather than allowing it to respire. Oxygen gas, produced during photosynthesis,

Table 1
Long-term fate of fossil fuel CO_2 with and without the temperature/CO_2 feedback

	Time scale (years)	% of fossil fuel CO_2 left in the atmosphere		Amplification factor (%)
		No *T* feedback	*T* feedback	
1000 Gtons				
Ocean invasion	300	15.2	17.8	17.2
After $CaCO_3$ neutralization	5000–8000	7.4	9.0	22.3
5000 Gtons				
Dissolution	300	26.5	31.0	17.2
$CaCO_3$ neutralization	5000–8000	8.2	10.5	28.2

is left behind when organic carbon is buried, resulting in a net source of O_2 to the atmosphere. Oxygen levels may also affect the ocean inventories of the nutrients PO_4^{3-}, NO_3^-, and Fe, limiting nutrients which serve to pace the biological cycle in the ocean, further feeding back to O_2. The extent of anoxia in the ocean, driven by ocean temperature, therefore has the potential to affect many aspects of the biosphere.

Walker [42] makes the observation that the ocean contains just enough PO_4^{3-} to bring the deep sea, on average, to the brink of anoxia. He proposes an analogy to a thermostat, which ought to have its switch contact close to closing, if the thermostat is regulating the temperature closely. The deep ocean is close to anoxic because if it went anoxic, it could easily generate more O_2 for the atmosphere, thereby pulling itself back to oxygenation.

Walker's story is complicated by the behavior of PO_4^{3-} in the ocean. O_2 in the deep ocean is consumed biologically, but the drawdown is limited by the availability of PO_4^{3-} to fuel photosynthesis in the surface ocean. (We assume that the ocean inventory of biologically available nitrogen is controlled, on geologic time scales, by the availability of PO_4^{3-}). Walker's thought experiment assumes that the surface ocean is saturated in O_2 and depleted in PO_4^{3-}. The PO_4^{3-} concentration of the deep ocean is close to the ocean mean (because it is a large reservoir). These assumptions yield

$$O_2(\text{deep ocean}) = O_2(\text{sat}) - (O/P)_{\text{plankton}} PO_4^{3-}(\text{mean})$$

where the term $(O/P)_{\text{plankton}}$ represents the oxygen demand for phytoplankton degradation, analogous to the Redfield ratio for N/P in plankton. The saturated O_2 concentration, O_2(sat), is defined by Henry's law

$$O_2(\text{sat}) = K_H(T)*pO_2(\text{atm})$$

where the equilibrium constant K_H decreases by about 25% with an increase in ocean temperature from 2 to 15 °C. Assuming hypothetically that the deep ocean approaches anoxia in the limit of a fully efficient biological pump, Walker derived the implication of these assumptions

$$pO_2(\text{atm}) = K_H(O/P)_{\text{plankton}} PO_4^{3-}(\text{mean})$$

and points out that this relation is nearly satisfied for today's ocean. The real deep ocean is not anoxic because not all of the upwelling PO_4^{3-} is utilized by phytoplankton, but it could be. The ocean contains just enough PO_4^{3-} to take the deep ocean to anoxia, neither much more nor less.

If we postulate that an ocean anoxia chemostat exists, maintaining this relationship through time, then we might speculate about the impact of a change in the O_2 solubility K_H. An increase in ocean temperature, driving a decrease in O_2 solubility, would have to be compensated by an increase in atmospheric O_2 or a decrease in ocean PO_4^{3-}. Several intriguing papers have been published on the interplay between O_2 and PO_4^{3-} [43–45]. In all of these models, anoxia in the ocean affects the burial of P, while the ocean inventory of P and the surface ocean O_2 concentration determine the O_2 concentration in the deep sea. Surface ocean O_2 depends on atmospheric pO_2 scaled by its solubility, which depends on temperature. An increase in temperature would decrease the solubility of oxygen, bringing anoxia that much closer to within reach of the biological pump. Oxygen solubility during the Cretaceous was about 25% lower than today. The effect of higher temperature, by itself, might have been to increase atmospheric pO_2 by approximately 25%, to offset the decrease in O_2 solubility. The physiology of Cretaceous insects [46] has lead to the speculation of higher O_2 concentrations at this time, but we have no reliable geochemical indications of atmospheric O_2 levels from this time [47].

4.3. Methane clathrates

Enormous amounts of methane exist in continental margin sediments of the ocean, frozen into cages of water ice in structures known as methane hydrates or clathrates. The total inventory of methane in the clathrate reservoir is poorly constrained, but has been estimated to exceed the inventory of extractable coal and other fossil fuels, by as much as a factor of 3 [48–51]. The distribution of methane clathrates in sediments of the ocean is limited by the temperature of the water and sediment columns (Fig. 5). At low pressure near the sea surface, the temperature of the overlying water is always too warm to support clathrate stability, except perhaps in the Arctic. Within the sediment

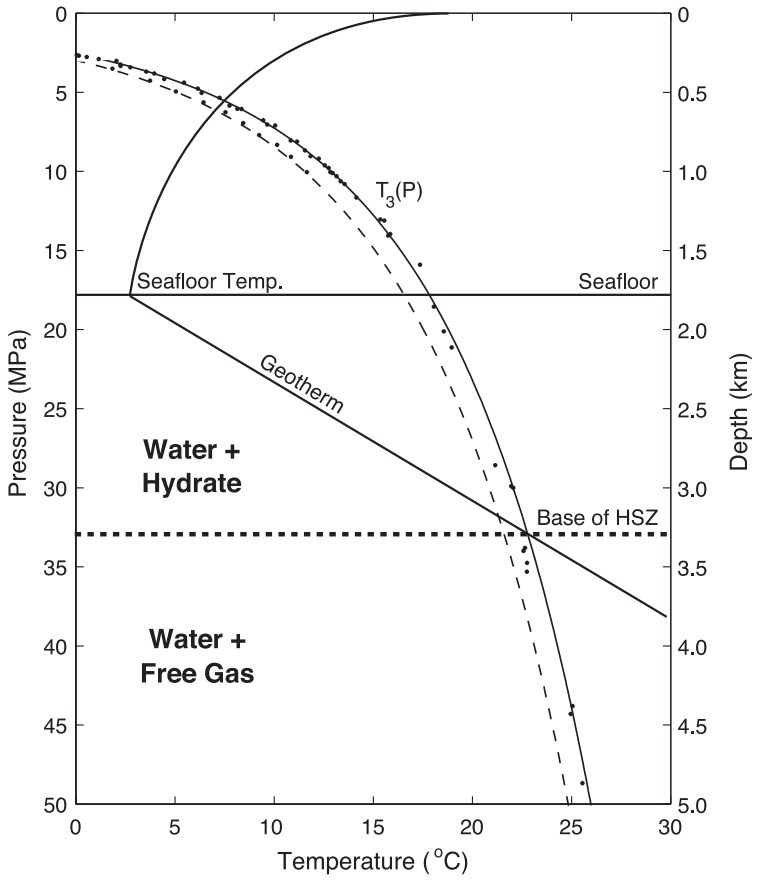

Fig. 5. Schematic illustration of temperature through the ocean and uppermost marine sediments. The temperature for clathrate stability, $T_3(P)$, increases with pressure (or depth). Experimental data for $T_3(P)$ in pure water (blue) and seawater (red) are extrapolated using a thermodynamic model [61]. A representative profile of temperature through the ocean intersects $T_3(P)$ at a depth of roughly 600 m, although clathrate is normally confined to the top few hundred meters of sediments. The base of the clathrate stability zone is defined by the intersection of the geotherm with $T_3(P)$. Adapted from Davie and Buffett [60].

column, the temperature increases with increasing depth along the geotherm. At depth in the sediment, the geotherm crosses the pressure-dependent clathrate stability temperature, demarking the lower bound for clathrate stability. The stability zone in the sediment increases with increasing water depth, but the organic carbon rain from the sea surface decreases toward the abyss. There is therefore a maximum abundance of clathrates at an intermediate depth range in the ocean, from 1 to 3 km. An increase in ocean temperature would decrease the thickness of the clathrate stability field [52], presumably decreasing the maximum inventory of clathrates in the global ocean.

Methane is a greenhouse gas, as is its oxidation product CO_2. The release of methane to the ocean or atmosphere during a transient warming has the potential to amplify the warming, creating a positive feedback analogous to that for the CO_2/T system described above. The two ingredients for the feedback are the temperature of the deep sea as driven by the radiative effect of the released carbon, and the sensitivity of the clathrate reservoir as a function of the temperature of the ocean. As for the O_2 and CO_2 systems, the time scales of the perturbations and responses play a major role in determining the behavior of the system.

4.3.1. Deep-ocean temperature response to clathrate methane release

If methane from decomposing clathrate manages to get to the atmosphere, its radiative impact will be 20 times stronger than CO_2 per molecule. However, the residence time of methane in the atmosphere, at present concentrations, is only around a decade, much shorter than the millennium time scale thermal response time of the deep sea. Therefore, the deep-ocean temperature rise associated with a short, catastrophic methane release depends on the dynamics of CO_2 rather than methane. The ocean carbon cycle model results presented above demonstrates that some fraction of any CO_2 added to the atmosphere/ocean reservoir remains in the atmosphere for order of 100 ky, limited by the time scale of the silicate weathering thermostat. A model of the PETM carbon cycle [53,54] predicted a 70-μatm rise in atmospheric pCO_2, assuming a 1000-Gton methane release spread over 10 ky. The atmospheric fraction of their clathrate carbon is 14%, broadly consistent with our model behavior, but we note that the atmospheric CO_2 signature would be higher if the methane release were larger (2000 Gtons is a more typical estimate) or faster (because $CaCO_3$ compensation neutralizes CO_2 if it has time). A 2000-Gton release in 1000 years might transiently increase pCO_2 by 600 Gtons, or about 300 μatm.

The radiative effect of the CO_2 increase depends on the initial pCO_2, because of the saturation of the infrared absorption bands of the CO_2. A doubling of the CO_2 concentration has roughly the same warming effect regardless of whether the doubling is from 100 to 200 μatm or from 1000 to 2000 μatm. The initial deep ocean temperature during the Paleocene, before the degassing event, was $\sim 8\,^{\circ}C$, suggesting an atmospheric pCO_2 much higher than today. If we add 100–200 μatm to an initial pCO_2 of say 1000 μatm, the radiative signature will be much too small to explain the $\sim 5\,^{\circ}C$ warming inferred from the $\delta^{18}O$ record. This suggests that the warming was driven externally, rather than simply by the clathrate decomposition event. On the other hand, the recovery from the warming parallels the recovery from the carbon isotope anomaly very closely, and the time scale for these recoveries are similar to the 100-ky time scale for silicate weathering neutralization of CO_2 and $\delta^{13}C$. Perhaps we are somehow underestimating the atmospheric pCO_2 response to the clathrate degassing, or its radiative impact.

4.3.2. Methane clathrate inventory as a function of ocean temperature

The other half of the clathrate/temperature system is the response of the clathrate inventory to changes in ocean temperature. The longest time scale in the system is the recharging of the clathrate reservoir after it is depleted, which takes place on a million-year time scale, limited by the rate of methane production and sediment advection. The real unknown is the time scale for a methane release in response to deep-ocean warming. A change in deep-ocean temperature could propagate through the order of 100-m-thick sedimentary clathrate zone in order 10^3 years. If methane clathrate dissociates rapidly, the released gas elevates the pressure of pore water in the sediments, potentially leading to failure and slumping of the marine sediments [55,56]. The potential for these is documented by numerous pockmarks and submarine landslides on the sea floor [57]. These would probably be local events rather than global, however, so they do not suggest a mechanism by which the entire global clathrate inventory might adjust itself in a catastrophic way.

Very different consequences are expected if the dissociation of methane clathrate occurs slowly. In this case, bubbles of methane gas can remain trapped in the sediments as the clathrate dissociates. Some of this methane dissolves into the surrounding pore water and is transported toward the seafloor by diffusion and fluid flow. Methane oxidation can follow either of two pathways. Reaction with sulfate, followed by sulfide precipitation, releases methane carbon in the form of HCO_3^-, ultimately provoking the precipitation of $CaCO_3$, which remains stably sequestered in the subsurface sediment column. Oxic methane oxidation in contrast releases carbon in the form of dissolved CO_2. On a thousand-year time scale, it makes little difference whether the CO_2 is produced in the atmosphere or the ocean; in either case, it will partition itself according to the proportions reflected in Table 1.

Isotopic data from the PETM indicate a degassing time scale between these two extremes. The isotopic signature of the methane reached shallow-

water $CaCO_3$ and terrestrial carbon deposits, which means that the methane did at least reach the ocean rather than precipitate as $CaCO_3$ at depth in the sediment [53]. The time scale for the $\delta^{13}C$ lightening (the release event) is estimated to be $\sim$ 10 ky [58].

4.3.3. Significance of the time scale asymmetry

The asymmetry in the time scales of buildup and decomposition of the methane clathrate reservoir has several interesting implications. One stems from the fact that buildup takes place on a longer time scale than the silicate weathering thermostat. The sequestration of carbon in the form of methane during the charging stage of the capacitor is therefore unable to affect the pCO_2 of the atmosphere very much, because that job belongs to the silicate weathering thermostat. Discharging the methane on the other hand is faster than silicate weathering, and therefore has the capacity to affect pCO_2 on time scales shorter than that for the silicate weathering thermostat.

Another interesting potential implication of the asymmetry of buildup and breakdown of the clathrate reservoir is that the inventory of methane over the glacial/interglacial cycles ought to reflect the ocean temperature maxima, not the minimum or time mean temperature, if the time scale for degassing is fast compared to a glacial cycle but the time scale for accumulation is slower. The implication for this would be that a future degassing adjustment, as earth's climate climbs into a greenhouse it has not seen in millions of years, might be larger than any methane release seen in response to the warming associated with the glacial termination.

5. Future directions

A remarkable observation from the geologic record is the relative stability of the temperature and atmospheric pO_2 through time, crucial to nurturing complex life and civilization. As mankind increasingly takes control of the biosphere, we need to understand the mechanisms responsible for this stability. An explanation of the glacial pCO_2 cycles, of which ocean temperature plays some part, will lend confidence to the forecast of the carbon cycle in the future. Our understanding of the physics responsible for the warm deep ocean in the early Cenozoic is incomplete, as is our understanding of the physics of warm climates generally. Research into the dynamics and stability of the methane hydrate reservoir is also in its infancy. The temperature of the ocean couples together the cycles and balances of CO_2, O_2, and methane, creating new feedbacks and interactions. Ultimately, many of the outstanding research problems and questions described in this paper will be relevant to forecasting the future trajectories of climate and geochemistry of the biosphere, although perhaps on time scales longer than are typically considered in global change deliberations.

Acknowledgements

We wish to thank Katharina Billups who provided Mg paleotemperature data, and Ken Caldeira, Andy Ridgwell, and Tom Guilderson for thorough, thoughtful and intelligent reviews. ***[AH]***

References

[1] R.J. Stouffer, S. Manabe, Equilibrium response of thermohaline circulation to large changes in atmospheric CO_2 concentration, Clim. Dyn. 20 (2003) 759–773.

[2] H.C. Urey, The thermodynamic properties of isotopic substances, J. Chem. Soc. (London) 297 (1947) 562–581.

[3] B.E. Bemis, H.J. Spero, J. Bijma, D.W. Lea, Reevaluation of the oxygen isotopic composition of planktonic foraminifera: experimental results and revised paleotemperature equations, Paleoceanography 13 (2) (1998) 150–160.

[4] N.J. Shackleton, Attainment of isotopic equilibrium between ocean water and the benthoic foraminifera genus *Unigerina*: isotopic changes in the ocean during the last glacial, Cent. Natl. Sci. Colloq. Int. 219 (1974) 203–209.

[5] D.P. Schrag, D.J. Depaolo, F.M. Richter, Reconstructing past sea-surface temperatures-correcting for diagenesis of bulk marine carbonate, Geochim. Cosmochim. Acta 59 (11) (1995) 2265–2278.

[6] P.N. Pearson, P.W. Ditchfield, J. Singano, K.G. Harcourt-Brown, C.J. Nicholas, R.K. Olsson, N.J. Shackleton, M.A. Hall, Warm tropical sea surface temperatures in the Late Cretaceous and Eocene epochs, Nature 413 (6855) (2001) 481–487.

[7] Y. Rosenthal, E.A. Boyle, N. Slowey, Temperature control on the incorporation of magnesium, strontium, fluorine, and cad-

mium into benthic foraminiferal shells from Little Bahama Bank: prospects for thermocline paleoceanography, Geochim. Cosmochim. Acta 61 (17) (1997) 3633–3643.
[8] T.A. Mashiotta, D.W. Lea, H.J. Spero, Glacial–interglacial changes in Subantarctic sea surface temperature and delta O-18-water using foraminiferal Mg, Earth Planet. Sci. Lett. 170 (4) (1999) 417–432.
[9] D.W. Lea, T.A. Mashiotta, H.J. Spero, Controls on magnesium and strontium uptake in planktonic foraminifera determined by live culturing, Geochim. Cosmochim. Acta 63 (16) (1999) 2369–2379.
[10] C.H. Lear, H. Elderfield, P.A. Wilson, Cenozoic deep-sea temperatures and global ice volumes from Mg/Ca in benthic foraminiferal calcite, Science 287 (5451) (2000) 269–272.
[11] K. Billups, D.P. Schrag, Paleotemperatures and ice volume of the past 27 Myr revisited with paired Mg/Ca and O-18/O-16 measurements on benthic foraminifera, Paleoceanography 17 (1).
[12] K. Billups, D.P. Schrag, Application of benthic foraminiferal Mg/Ca ratios to questions of Cenozoic climate change, Earth Planet. Sci. Lett. 209 (1–2) (2003) 181–195.
[13] P.A. Martin, D.W. Lea, Y. Rosenthal, N.J. Shackleton, M. Sarnthein, T. Papenfuss, Quaternary deep sea temperature histories derived from benthic foraminiferal Mg/Ca, Earth Planet. Sci. Lett. 198 (1–2) (2002) 193–209.
[14] J.C. Zachos, M. Pagani, L. Sloan, E. Thomas, K. Billups, Trends, rhythms, and aberrations in global climate 65 Ma to Present, Science 292 (2001) 686–693.
[15] J.C. Zachos, J.R. Breza, S.W. Wise, Early Oligocene ice-sheet expansion on Antarctica—stable isotope and sedimentological evidence from Kerguelen Plateau, Southern Indian-Ocean, Geology 20 (6) (1992) 569–573.
[16] P. Martin, Evidence for the role of deep sea temperatures in glacial climate and carbon cycle, Paleoceanography, in press.
[17] D.P. Schrag, G. Hampt, D.W. Murray, Pore fluid constraints on the temperature and oxygen isotopic composition of the glacial ocean, Science 272 (1996) 3385–3388.
[18] J.F. Adkins, K. McIntyre, D.P. Schrag, The salinity, temperature, and d18O of the glacial deep ocean, Science 298 (2002) 1769–1773.
[19] N.J. Shackleton, The 100,000-year ice-age cycle identified and found to lag temperature, carbon dioxide, and orbital eccentricity, Science 289 (5486) (2000) 1897–1902.
[20] J. Chappell, Sea level changes forced ice breakouts in the Last Glacial cycle: new results from coral terraces, Quat. Sci. Rev. 21 (10) (2002) 1229–1240.
[21] M. Huber, L.C. Sloan, Heat transport, deep waters, and thermal gradients: coupled simulation of an Eocene greenhouse climate, Geophys. Res. Lett. 28 (18) (2001) 3418–3484.
[22] R. Zhang, M. Follows, J. Marshall, Mechanisms of thermohaline mode switching with application to warm equable climates, J. Climate 15 (2001) 2056–2072.
[23] R. Zhang, M.J. Follows, J.P. Grotzinger, J. Marshall, Could the late Permian deep ocean have been anoxic? Paleoceanography 16 (3) (2001) 317–329.
[24] A. Ganopolski, S. Rahmstorf, V. Petoukhov, M. Claussen, Simulation of modern and glacial climates with a coupled global model of intermediate complexity, Nature 371 (1998) 323–326.
[25] C.D. Hewitt, A.J. Broccoli, J.F.B. Mitchell, R.J. Stouffer, A coupled model study of the last glacial maximum: was part of the North Atlantic relatively warm? Geophys. Res. Lett. 28 (2001) 1571–1574.
[26] J.C. Duplessy, N.J. Shackleton, R.G. Fairbanks, L. Labeyrie, D. Oppo, N. Kallel, Deepwater source variations during the last climatic cycle and their impact on the global deepwater circulation, Paleoceanography 3 (1988) 343–360.
[27] S.-I. Shin, Z. Liu, B. Otto-Bliesner, E.C. Brady, J.E. Kutzbach, S.P. Harrison, A simulation of the Last Glacial Maximum using the NCAR-CCSM, Clim. Dyn. 20 (2003) 127–151.
[28] R.J. Stouffer, S. Manabe, Response of a coupled ocean-atmosphere model to increasing atmospheric carbon dioxide: sensitivity to the rate of increase, J. Climate 12 (8) (1999) 2224–2237.
[29] D.E. Archer, E. Maier-Reimer, Effect of deep-sea sedimentary calcite preservation on atmospheric CO_2 concentration, Nature 367 (1994) 260–264.
[30] D. Archer, H. Kheshgi, E. Maier-Riemer, Multiple timescales for neutralization of fossil fuel CO_2, Geophys. Res. Lett. 24 (1997) 405–408.
[31] D. Archer, H. Kheshgi, E. Maier-Reimer, Dynamics of fossil fuel CO2 neutralization by marine $CaCO_3$, Glob. Biogeochem. Cycles 12 (1998) 259–276.
[32] W.H. Berger, Increase of carbon dioxide in the atmosphere during deglaciation: the coral reef hypothesis, Naturwissenschaften 69 (1982) 87–88.
[33] J.R. Petit, J. Jouzel, D. Raynaud, N.I. Barkov, J.-M. Barnola, I. Basile, M. Bender, J. Chappellaz, M. Davis, G. Delaygue, M. Delmotte, V.M. Kotlyakov, M. Legrand, V.Y. Lipenkov, C. Lorius, L. Pepin, C. Ritz, E. Saltzman, M. Stievenard, Climate and atmospheric history of the past 420,000 years from the Vostok ice core, Antarctica, Nature 399 (1999) 429–436.
[34] D.E. Archer, A. Winguth, D. Lea, N. Mahowald, What caused the glacial/interglacial atmospheric pCO_2 cycles? Rev. Geophys. 38 (2000) 159–189.
[35] J.C.G. Walker, P.B. Hays, J.F. Kasting, A negative feedback mechanism for the long-term stabilization of Earth's surface temperature, J. Geophys. Res. 86 (1981) 9776–9782.
[36] R.A. Berner, A.C. Lasaga, R.M. Garrels, The carbonate-silicate geochemical cycle and its effect on atmospheric carbon dioxide over the past 100 million years, Am. J. Sci. 283 (1983) 641–683.
[37] R.A. Berner, GEOCARB II: a revised model of atmospheric CO_2 over Phanerozoic time, Am. J. Sci. 294 (1994) 56–91.
[38] R.A. Berner, Z. Kothavala, GEOCARB III: a revised model of atmospheric CO_2 over Phanerozoic time, Am. J. Sci. 301 (2) (2001) 182–204.
[39] J. Kennett, B. Ingram, A 20,000-year record of ocean circulation and climate change from the Santa Barbara basin, Nature 377 (1995) 510–514.
[40] R.S. Ganeshram, T.F. Pedersen, S.E. Calvert, J.W. Murray, Large changes in oceanic nutrient inventories from glacial to interglacial periods, Nature 376 (1995) 755–758.
[41] M.A. Altabet, R. Francois, D.W. Murray, W.L. Prell, Climate-

related variations in denitrification in the Arabian Sea from sediment 15N/14N ratios, Nature 373 (1995) 506–509.
[42] J.C.G. Walker, Evolution of the Atmosphere, Macmillan, New York, 1977, 318 pp.
[43] P.V. Cappellen, E. Ingall, Redox stabilization of the atmosphere and oceans by phosphorus-limited marine productivity, Science 271 (1996) 493–495.
[44] T.M. Lenton, A.J. Watson, Redfield revisited: 1. Regulation of nitrate, phosphate, and oxygen in the ocean, Glob. Biogeochem. Cycles 14 (2000) 225–248.
[45] I.C. Handoh, T.M. Lenton, Periodic mid-Cretaceous ocean anoxic events linked by oscillations of the phosphorus and oxygen biogeochemical cycles, Glob. Biogeochem. Cycles 17 (2003) doi:10.1029/2003GB0022039.
[46] J.B. Graham, R. Dudley, N.M. Aguilar, C. Gans, Implications of the late Palaeozoic oxygen pulse for physiology and evolution, Nature 375 (1995) 117–120.
[47] R.A. Berner, Atmospheric oxygen over Phanerozoic time, Proc. Natl. Acad. Sci. U. S. A. 96 (1999) 10955–10957.
[48] K.A. Kvenvolden, Methane hydrate—a major reservoir of carbon in the shallow geosphere, Chem. Geol. 71 (1–3) (1988) 41–51.
[49] G. MacDonald, Role of methane clathrates in past and future climates, Clim. Change 16 (1990) 247–281.
[50] V. Gornitz, I. Fung, Potential distribution of methane hydrate in the world's oceans, Glob. Biogeochem. Cycles 8 (1994) 335–347.
[51] L.D.D. Harvey, Z. Huang, Evaluation of the potential impact of methane clathrate destabilization on future global warming, J. Geophys. Res. 100 (1995) 2905–2926.
[52] G.R. Dickens, The potential volume of oceanic methane hydrates with variable external conditions, Org. Geochem. 32 (2001) 1179–1193.
[53] G.R. Dickens, Modeling the global carbon cycle with a gas hydrate capaciter: significance for the latest Paleocene thermal maximum, in: Natural Gas Hydrates: Occurrence, Distribution and Detection, AGU Geophys. Monogr. 124 (2001) 19–38.
[54] J.C.G. Walker, J.F. Kasting, Effects of fuel and forest conservation on future levels of atmospheric carbon dioxide, Palaeogeogr. Palaeoclimatol. Palaeoecol. (Glob. Planet. Change Sect.) 97 (1992) 151–189.
[55] R.D. McIver, Role of naturally occurring gas hydrates in sediment transport, AAPG Bull. 66 (1982) 789–792.
[56] R.E. Kayen, H.J. Lee, Pleistocene slope instability of gas hydrate-laden sediment of Beaufort Sea margin, Marine Geotech. 10 (1991) 125–141.
[57] M. Hovland, A.G. Judd, Seabed Pockmarks and Seepages, Graham and Trotman, London, 1988.
[58] G.R. Dickens, Rethinking the global carbon cycle with a large, dynamic and microbially mediated gas hydrate capacitor, Earth Planet. Sci. Lett. 213 (2003) 169–183.
[59] L.D. Laberyie, J.C. Duplessy, P.L. Blanc, Variations in mode of formation and temperature of oceanic deep waters over the past 125,000 years, Nature 327 (1987) 477–482.
[60] M.K. Davie, B.A. Buffett, Sources of methane for marine gas hydrate: inferences from a comparison of observations and numerical models, Earth Planet. Sci. Lett. 206 (1–2) (2003) 51–63.
[61] E.D. Sloan, Clathrate Hydrates of Natural Gas, Marcel Dekker, New York, 1988.

David Archer is a professor in the Geophysical Sciences Department at the University of Chicago, where he studies the carbon cycle in the ocean and in deep-sea sediments, and its relation to global climate.

Pamela Martin is an assistance professor in the Geophysical Sciences Department at the University of Chicago. Her research broadly focuses on reconstructing changes in deep-ocean temperature, chemistry, and circulation to understand oceanic controls on climate change. She is interested in the links between ocean biogeochemical cycles, atmospheric carbon dioxide and climate change on time scales ranging from orbital variations (hundreds of thousands of years) to anthropogenic variations (decades to millennium). She makes measurements of the chemical composition of fossils to document climate changes in the geologic record and use numerical models to investigate the ocean's role in the climate system.

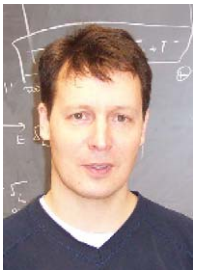

Bruce Buffett is a professor in the Geophysical Sciences Department at the University of Chicago. His research deals with dynamical processes in the Earth's interior. This can include mantle convection, plate tectonics, and the generation of the Earth's magnetic field. A central theme that connects these processes is the thermal and compositional evolution of the Earth because it affects the energy which is available to drive the internal dynamics of the planet. I attempt to understand the structure, dynamics and evolution of the Earth's interior using theoretical models in combination with geophysical observations.

Victor Brovkin, is a Post-Doc at Potsdam Institute for Climate Impact Research, Postdam, Germany. He has 10 years experience in biospheric modelling on a global scale with focus on developing of vegetation dynamics, terrestrial and oceanic carbon cycle models for Earth System Models of Intermediate Complexity (EMICs). His main scientific interests include stability analysis of climate–vegetation system, effect of deforestation on climate system, and integration of terrestrial and marine components of the global carbon cycle.

Stefan Rahmstorf is a research scientist at the Potsdam Institute for Climate Impact Research and a professor at the University of Potsdam. His research team studies the role of the oceans in climate change, in the past (e.g, during the last Ice Age), in the present and for a further global warming.

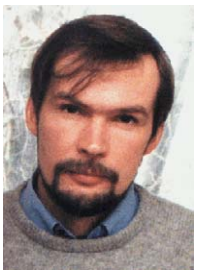

Andrey Ganopolski obtained his MS and PhD degrees in geophysics at the Moscow State University. Since 1994, he is research scientist at the Potsdam Institute for Climate Impact Research. His work focuses on climate modelling, climate predictions and studying of the past climate changes.